


## Article

# Assessing PM<sub>2.5</sub> Dynamics and Source Contributions in Southwestern China: Insights from Winter Haze Analysis

Hui Guan <sup>1,\*</sup> , Ziyun Chen <sup>1,2</sup>, Jing Tian <sup>1</sup> and Huayun Xiao <sup>3</sup>

<sup>1</sup> State Key Laboratory of Environmental Geochemistry, Institute of Geochemistry, Chinese Academy of Sciences, Guiyang 550081, China; chenziyun@mail.gyig.ac.cn (Z.C.); tianjing@mail.gyig.ac.cn (J.T.)

<sup>2</sup> University of Chinese Academy of Sciences, Beijing 100049, China

<sup>3</sup> School of Agriculture and Biology, Shanghai Jiao Tong University, Shanghai 200240, China; xiaohuayun@sjtu.edu.cn

\* Correspondence: guanhui@mail.gyig.ac.cn

**Abstract:** Despite enhancements in pollution control measures in southwestern China, detailed assessments of PM<sub>2.5</sub> dynamics following the implementation of the Clean Air Action remain limited. This study explores the PM<sub>2.5</sub> concentrations and their chemical compositions during the winter haze period of 2017 across four major urban centers—Chengdu, Chongqing, Guiyang, and Kunming. Significant variability in mean PM<sub>2.5</sub> concentrations was observed: Chengdu (71.8 μg m<sup>-3</sup>) and Chongqing (53.3 μg m<sup>-3</sup>) recorded the highest levels, substantially exceeding national air quality standards, while Guiyang and Kunming reported lower concentrations, suggestive of comparatively milder pollution. The analysis revealed that sulfate, nitrate, and ammonium (collectively referred to as SNA) constituted a substantial portion of the PM<sub>2.5</sub> mass—47.2% in Chengdu, 62.2% in Chongqing, 59.9% in Guiyang, and 32.0% in Kunming—highlighting the critical role of secondary aerosol formation. The ratio of NO<sub>3</sub><sup>-</sup>/SO<sub>4</sub><sup>2-</sup> and nitrogen oxidation ratio to sulfur oxidation ratio (NOR/SOR) indicate a significant transformation of NO<sub>2</sub> under conditions of heavy pollution, with nitrate formation playing an increasingly central role in the haze dynamics, particularly in Chengdu and Chongqing. Utilizing PMF for source apportionment, in Chengdu, vehicle emissions were the predominant contributor, accounting for 33.1%. Chongqing showed a similar profile, with secondary aerosols constituting 36%, followed closely by vehicle emissions. In contrast, Guiyang's PM<sub>2.5</sub> burden was heavily influenced by coal combustion, which contributed 46.3%, reflecting the city's strong industrial base. Kunming presented a more balanced source distribution. Back trajectory analysis further confirmed the regional transport of pollutants, illustrating the complex interplay between local and distant sources. These insights underscore the need for tailored, region-specific air quality management strategies in southwestern China, thereby enhancing our understanding of the multifaceted sources and dynamics of PM<sub>2.5</sub> pollution amidst ongoing urban and industrial development.

**Keywords:** PM<sub>2.5</sub> analyses; water-soluble ions; secondary aerosols; source apportionment; PMF



**Citation:** Guan, H.; Chen, Z.; Tian, J.; Xiao, H. Assessing PM<sub>2.5</sub> Dynamics and Source Contributions in Southwestern China: Insights from Winter Haze Analysis. *Atmosphere* **2024**, *15*, 855. <https://doi.org/10.3390/atmos15070855>

Academic Editor: Daekeun Kim

Received: 26 June 2024

Revised: 11 July 2024

Accepted: 17 July 2024

Published: 19 July 2024



**Copyright:** © 2024 by the authors. Licensee MDPI, Basel, Switzerland. This article is an open access article distributed under the terms and conditions of the Creative Commons Attribution (CC BY) license (<https://creativecommons.org/licenses/by/4.0/>).

## 1. Introduction

Amid rapid economic development, population growth, industrial expansion, and urbanization over recent decades, China has confronted severe air pollution challenges. Notably, particulate matter with an aerodynamic diameter of less than 2.5 μm (PM<sub>2.5</sub>) has increasingly become a focal point due to its significant adverse effects on human health [1–4], its role in visibility degradation [5–7], and its potential impact on climate change [8,9]. Furthermore, PM<sub>2.5</sub> is crucial in haze formation, primarily resulting from anthropogenic emissions and gas-to-particle conversion processes [10,11].

Extensive research has revealed that PM<sub>2.5</sub> primarily consists of water-soluble inorganic ions, carbonaceous species, and elements such as Ca, Si, Ti, Mg, Zn, and Fe. These particles originate either directly from natural and anthropogenic sources—including

biomass burning, vehicle exhaust fumes, and industrial activities—or as secondary pollutants through heterogeneous chemical reactions [12–19]. However, the focus of such studies has predominantly been on economically developed urban clusters such as the Beijing–Tianjin–Hebei (BTH) region, Central China area, Yangtze River Delta (YRD), and Pearl River Delta (PRD) [5,20–26], with limited studies addressing the situation in southwestern China.

This research focuses on Chengdu, Chongqing, Guiyang, and Kunming—the largest cities in southwestern China, where air pollution varies considerably. Chengdu, known for its severe pollution exacerbated by unfavorable atmospheric conditions and high humidity [15], contrasts sharply with Kunming, where such issues are minimal due to favorable meteorological conditions. Similarly, Chongqing’s mountainous terrain facilitates pollutant accumulation [27,28], and Guiyang suffers from significant pollution due to extensive coal combustion [29]. The PM<sub>2.5</sub> pollution in southwestern cities shows significant seasonal and spatial variations, influenced by multiple sources and weather conditions. Major sources include secondary inorganic aerosols, vehicle emissions, coal combustion, and industrial emissions [30,31]. Local emissions and regional transport are critical, with key components like sulfate, nitrate, and ammonium in Guiyang [32–34]. Despite reductions post-2013 due to strict controls, local emissions still dominate air quality impacts [35,36]. These studies provide important insights into PM<sub>2.5</sub> pollution and control strategies in these cities.

Coal burning produces more than 70% of China’s electricity, and is still widely used for domestic heating and cooking, especially in cities in the relatively underdeveloped southwestern China [37]. Most of the limited studies about particulate pollution in southwestern China have attributed the main source of PM<sub>2.5</sub> mass to coal burning [15,27,38,39]. Over the last decade, however, most of small-sized mills and mines as well as workshops with heavy pollution have been forced to shut down and some heavy polluting industries were relocated from downtown to the suburbs. And 90% of the city residents have replaced coal with natural gas now. After the implementation of the Clean Air Action Plan in 2013, the PM<sub>2.5</sub> levels in most of the cities of southwestern China have shown remarkable decreases (i.e., 129  $\mu\text{g}\cdot\text{m}^{-3}$  for Chongqing in 2006 and 87.7  $\mu\text{g}\cdot\text{m}^{-3}$  in 2017) [39–41]. Meanwhile, the number of vehicles in southwestern China, especially in Chengdu and Chongqing, has dramatically increased like the rest of China. All these changes show a turning point has been reached for the chemical composition and sources of PM<sub>2.5</sub> in southwestern China. Unfortunately, although some studies on particulate pollution have been carried out during these years, detailed data relating to PM<sub>2.5</sub> in these cities are very scarce, especially those collected in Guiyang and Kunming.

This study aimed to assess the PM<sub>2.5</sub> levels in these cities during the winter haze period of 2017, exploring changes in chemical composition and pollution sources in the context of shifting energy consumption and rapid urban development. The innovative nature of this work lies in its comprehensive analysis across multiple urban centers, using detailed chemical composition and advanced source apportionment techniques. Through detailed PM<sub>2.5</sub> measurements and the application of the Positive Matrix Factorization (PMF) receptor model, we quantified source contributions and offer insights into the evolving air quality dynamics of southwestern China. This comprehensive analysis not only bridges the existing research gap but also enhances our understanding of regional air pollution management strategies. The delay in presenting these results is due to extensive data analysis and coordination challenges. Despite the delay, the findings are highly relevant and contribute significantly to the understanding of PM<sub>2.5</sub> pollution in southwestern China.

## 2. Experiments

### 2.1. Site Description

The sampling sites strategically selected for this study are located across four major urban centers in southwestern China, as indicated in Figure 1. Each site was selected to represent the unique environmental and urban characteristics of its respective city, facilitating a comprehensive analysis of regional air quality.

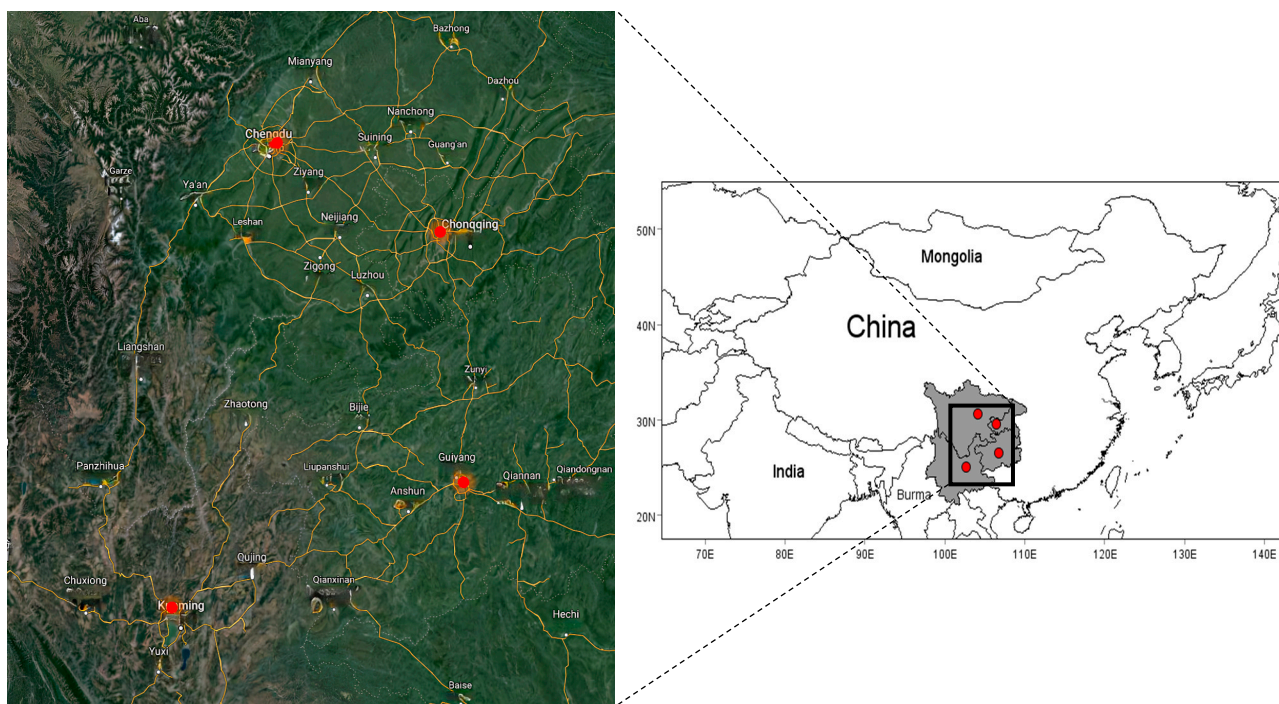


**Figure 1.** Locations of sampling sites in southwestern China.

**Chengdu:** The provincial capital of Sichuan Province hosts the sampling site on the roof of a six-floor building (20 m above ground) at the Chengdu University of Technology. Positioned at coordinates  $104^{\circ}15' E$ ,  $30^{\circ}68' N$ , this site is surrounded by multiple urban roadways, capturing the typical traffic-related air pollution characteristics of Chengdu.

**Chongqing:** Situated near the eastern border of the Sichuan Basin, Chongqing's sampling site is located on the Chongqing University (CU) campus, in the heart of the city at coordinates  $106^{\circ}48' E$ ,  $29^{\circ}57' N$ . The sampling instruments were placed on the roof of a five-story building, approximately 15 m above ground, providing exposure to the urban atmosphere without obstruction.

**Guiyang:** As the capital of Guizhou Province, Guiyang presents a diverse urban setting. The sampling location is set atop an apartment building approximately 10 m high, on the campus of the Institute of Geochemistry of the Chinese Academy of Sciences, positioned at  $106^{\circ}73' E$ ,  $26^{\circ}57' N$ . This central city location lies within a busy commercial, traffic, and residential area, making it ideal for assessing urban air pollutants.

**Kunming:** The sampling site in Kunming, the capital of Yunnan Province, is located at the Lianhua campus of the Kunming University of Science and Technology ( $102^{\circ}42' E$ ,  $25^{\circ}04' N$ ). The  $PM_{2.5}$  sampler was deployed on the rooftop of a 15 m tall building within a zone that blends residential and commercial activities. This setup is intended to monitor air quality in a mixed-use area that reflects both residential and business activities.

## 2.2. Field Sampling

From 15 November to 15 December 2017, a comprehensive field sampling campaign was conducted across the four designated urban sites. To provide a more comprehensive picture of seasonal variations in air quality, future studies should aim to increase the frequency of  $PM_{2.5}$  sample collection to cover all seasons of the year. This will help identify critical periods of pollution and enhance the robustness of air quality management strategies. During this period, a total of 120  $PM_{2.5}$  samples were systematically collected to ensure synchronicity and comparability across locations.

$PM_{2.5}$  samples were collected daily at 09:30 AM over a continuous 24 h period using the high-flow-rate KC-1000 sampler (Qingdao Laoshan Applied Technology Research

Institute, Qingdao, China), operating at a flow rate of  $1.05 \pm 0.03 \text{ m}^3/\text{min}$ . The particulate matter was captured on pre-baked quartz fiber filters (QFFs) with a diameter of 90 mm, model 2500 QAT-UP from Pall Life Sciences (Pall Corporation, Port Washington, NY, USA). To avoid contamination and ensure the accuracy of the sample measurements, all QFFs were pre-baked at  $450 \text{ }^\circ\text{C}$  for four hours prior to their use.

Following the collection, each filter was conditioned for 24 h in a controlled environment at a constant temperature ( $20 \pm 1 \text{ }^\circ\text{C}$ ) and humidity ( $40 \pm 1\%$ ) before and after sampling, to ensure precise weight measurements. The weighing was performed using an analytical balance from Mettler Toledo (Columbus, OH, USA) with a sensitivity of 0.1 mg. Post-collection, all samples were stored at  $-18 \text{ }^\circ\text{C}$  to preserve their chemical integrity until analysis.

In conjunction with the particulate matter sampling, meteorological data for each site were gathered from the National Meteorological Information Center, which included parameters such as temperature, atmospheric pressure, relative humidity, wind speed, and precipitation. The link for the data source is [National Meteorological Information Center] <http://data.cma.cn/en> (accessed on 13 September 2018) (Figure 2). Additionally, spatial distribution data concerning geopotential height were obtained from the archived meteorological databases of NOAA's Air Resources Laboratory ([ARL] (<https://www.ready.noaa.gov> (accessed on 13 September 2018))).

This meticulous approach to sample collection and handling ensures the reliability of the data, which is critical for analyzing the spatiotemporal variations and source apportionment of  $\text{PM}_{2.5}$  in these urban environments.

### 2.3. Chemical Analysis

Ion chromatography (IC) (ICS-3000, Dionex, Sunnyvale, CA, USA) was used to determine the concentrations of six anion ( $\text{F}^-$ ,  $\text{Cl}^-$ ,  $\text{NO}_3^-$ ,  $\text{SO}_4^{2-}$ ,  $\text{Br}^-$ , and  $\text{NO}_2^-$ ) and five cation ( $\text{Na}^+$ ,  $\text{K}^+$ ,  $\text{Ca}^{2+}$ ,  $\text{Mg}^{2+}$ , and  $\text{NH}_4^+$ ) species in one-quarter of the QFFs. A Dionex separator column of AS11-HC with KOH eluent was used for anion analysis, and a cation analytical column of CS12A and an eluent of 20 mM methyl sulfonic acid was used to analyze inorganic cations. Details of the IC method are described in [42] and [43]. The detection limits (DLs) of  $\text{Na}^+$ ,  $\text{NH}_4^+$ ,  $\text{K}^+$ ,  $\text{Ca}^{2+}$ ,  $\text{Mg}^{2+}$ ,  $\text{F}^-$ ,  $\text{Cl}^-$ ,  $\text{NO}_3^-$ ,  $\text{SO}_4^{2-}$ ,  $\text{Br}^-$ , and  $\text{NO}_2^-$  were 0.001, 0.0012, 0.0018, 0.0009, 0.0025, 0.0038, 0.0051, 0.022, 0.012, 0.033, and  $0.021 \mu\text{g m}^{-3}$ , respectively. A careful quality assurance and quality control (QA/QC) procedure was applied. Standard solution was obtained from the National Research Center of Certified Reference Materials, China. Blank and standard samples were repeated every ten samples.

For the quantification of carbonaceous species in  $\text{PM}_{2.5}$  samples, a thermal/optical reflectance (TOR) method was utilized, following the protocol established by the National Institute for Occupational Safety and Health (NIOSH Method 5040). Samples were collected on quartz fiber filters, which are suitable for absorbing organic compounds without chemical interference.

In the analysis process, filters were subjected to a stepwise heating program in a carbon analyzer. The program first heats the sample in a non-oxidizing helium atmosphere to volatilize and oxidize organic carbon. The temperature is then increased under an oxidizing atmosphere to convert elemental carbon into  $\text{CO}_2$ . The evolved  $\text{CO}_2$  is detected and quantified by a flame ionization detector (FID).

### 2.4. Backward Trajectories Analysis

Backward trajectories are used to determine the long-distance transport of atmospheric pollutants and regional source areas by the program of TrajStat (version 1.4.7) [44]. FNL global analysis data are the input data, generated by the National Centers for Environmental Prediction (NCEP) model and processed by the Global Data Assimilation System (GDAS) (<https://www.ready.noaa.gov/HYSPLIT.php> (accessed on 9 February 2023)). Trajectories extending 3 days (72 h) into the past were estimated per day (0, 6, 12, 18 UTC) for the period from 15 November to 15 December 2017. Each trajectory was calculated at 500 m



above the ground. To determine the pollutant sources, five typical types of trajectories were classified using the hierarchical clustering method [45].

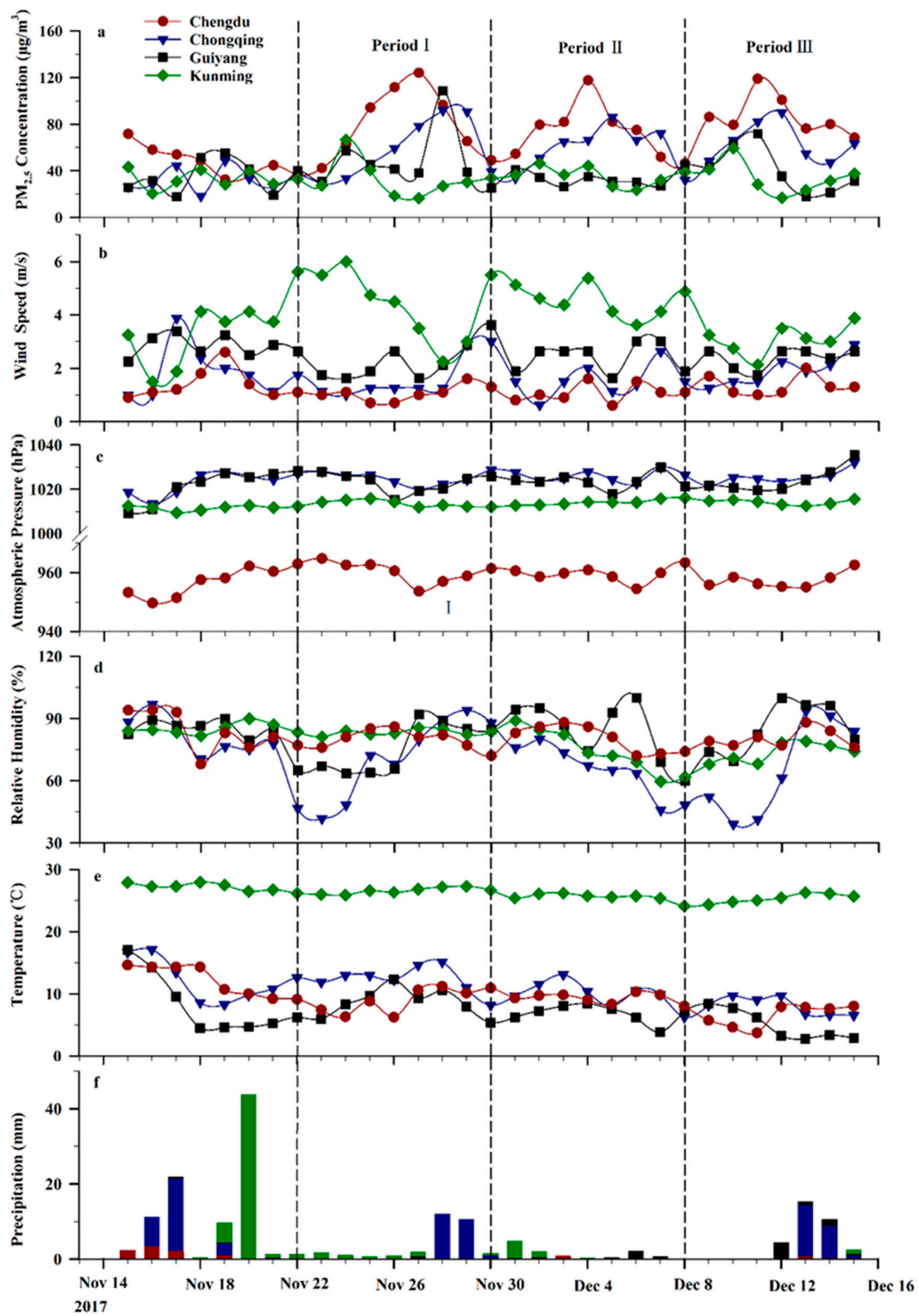


Figure 2. PM<sub>2.5</sub> mass concentrations (a) and meteorological conditions (WS (b), Pres. (c), RH (d), Temp. (e) and Pres. (f)) during sampling periods.

### 2.5. Positive Matrix Factorization Model

Receptor models are used to quantify the contributions of sources based on their composition or fingerprints [46]. The PMF is an effective source apportionment receptor model that does not require source profiles prior to analysis and has no limitation on source numbers [43,47]. To enhance the accuracy of source identification and their respective contributions, integrating further source apportionment models, such as the Chemical Mass Balance (CMB), is recommended. Utilizing multiple models can provide a more detailed and accurate identification of PM<sub>2.5</sub> sources, enhancing the reliability of source apportionment results and informing more effective mitigation policies. Future research should consider the application of the CMB model alongside PMF to validate and refine the source apportionment findings presented in this study. The principles of the PMF model have been discussed in detail elsewhere [48]. In our study, EPA PMF 5.0 was used to determine source apportionment of each major ion. The final PMF solution was determined by choosing the most stable results with respect to different input options and choosing the one with the most physically interpretable profiles and stable/minimal Q value.

## 3. Results and Discussion

### 3.1. Spatial–Temporal Variations in PM<sub>2.5</sub> Mass Concentrations

The spatial and temporal distribution of PM<sub>2.5</sub> concentrations across the four study sites during the sampling period is summarized in Table 1a,b. Average PM<sub>2.5</sub> concentrations, expressed as mean  $\pm$  standard deviation ( $\mu\text{g m}^{-3}$ ), varied significantly among the locations: Chengdu (CD)  $71.8 \pm 25.8$ , Chongqing (CQ)  $53.3 \pm 21.7$ , Guiyang (GY)  $39.4 \pm 18.2$ , and Kunming (KM)  $33.8 \pm 11.2$ . This gradient demonstrates a clear pattern of CD > CQ > GY > KM, with all sites exceeding the China PM<sub>2.5</sub> Class II air quality standard of  $35 \mu\text{g m}^{-3}$  (GB 3095-2012 [49]), except for KM. Specifically, PM<sub>2.5</sub> levels in CD were more than double this limit, while those in CQ exceeded it by more than 1.5 times, and Guiyang slightly surpassed this threshold.

During the winter haze period, the mean PM<sub>2.5</sub> concentrations in CD aligned with those recorded at Shangdianzi, a northern China Atmospheric Watch Station ( $71.8 \mu\text{g m}^{-3}$ ), yet were lower than the concentrations observed in major northern urban centers such as Beijing ( $135 \mu\text{g m}^{-3}$ ) and Tianjin ( $141.0 \mu\text{g m}^{-3}$ ) [50]. Conversely, the PM<sub>2.5</sub> levels in CQ were comparable to those in Fuzhou ( $59.8 \mu\text{g m}^{-3}$ ) [51]. Guiyang and Kunming exhibited concentrations lower than other Chinese cities but higher than rural and background sites in Europe and America during the same period, such as a central Mediterranean coastal site ( $13.9 \mu\text{g m}^{-3}$ ) [52] and a rural UK site ( $10.5 \mu\text{g m}^{-3}$ ) [53].

Figure 3a illustrates the annual variations in winter PM<sub>2.5</sub> concentrations in CD and CQ from 2010 to 2017 [15,28,31,40,54–56]. The data indicate effective control of PM<sub>2.5</sub> pollution in these cities post-2010. Although a peak in 2015 saw levels rise to  $149.6 \mu\text{g m}^{-3}$  in CD, the concentrations in 2014 and 2016 were significantly reduced to approximately  $113.5$  and  $101.0 \mu\text{g m}^{-3}$ , respectively. This decreasing trend in PM<sub>2.5</sub> concentrations is attributed to stringent emission reduction measures implemented in both cities.

Additionally, Figure 2 presents the relationship between PM<sub>2.5</sub> mass concentrations and meteorological parameters (RH, STP, TEMP, WS, and PRCP). Pollution episodes across all cities exhibited a periodic cycle of 7–8 days, as reflected in the fluctuations in PM<sub>2.5</sub> concentrations. Typically, the PM<sub>2.5</sub> concentration increased from less than  $50 \mu\text{g m}^{-3}$  (clean) to  $50$ – $80 \mu\text{g m}^{-3}$  (transition) and exceeded  $80 \mu\text{g m}^{-3}$  during heavily polluted episodes. Generally, PM<sub>2.5</sub> levels are influenced by emissions, transportation, chemical transformations, and deposition processes, all closely linked to meteorological conditions [57]. Notably, higher PM<sub>2.5</sub> concentrations were associated with lower wind speeds (WS), temperatures (TEMP), and precipitation (PRCP), which likely hindered the dispersion and removal of pollutants. For instance, Kunming experienced lower PM<sub>2.5</sub> concentrations, benefiting from more favorable meteorological conditions, unlike Chengdu and Chongqing, where the opposite was true.

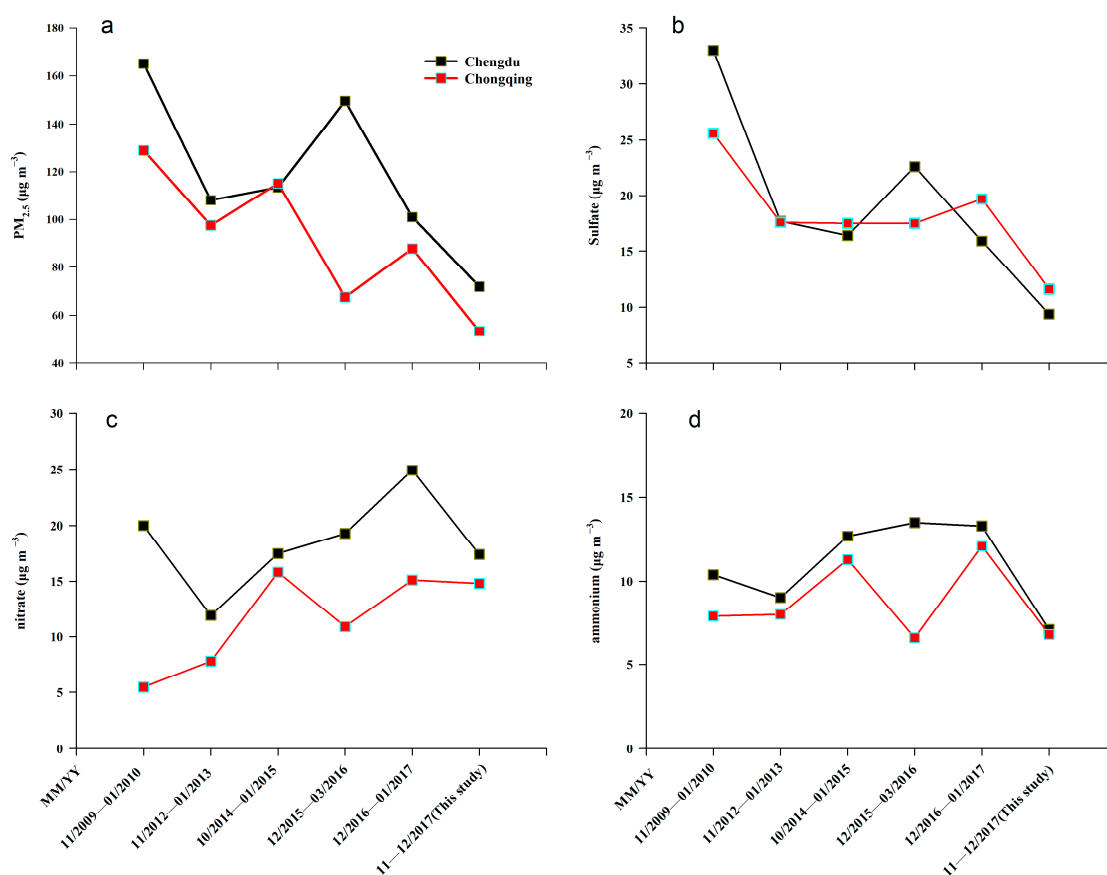
**Table 1.** (a) Concentrations and (±) standard deviations of chemical components during the sampling period and different haze periods in Chengdu and Congqing. (b) Concentrations and (±) standard deviations of chemical components during the sampling period and different haze periods in Guiyang and Kunming.

(a)								
	Chengdu (CD)				Chongqing (CQ)			
	Sampling Period	Polluted	Transition	Clean	Sampling Period	Polluted	Transition	Clean
PM <sub>2.5</sub> /μg m <sup>-3</sup>	71.8 ± 25.8	99.4 ± 16.3	66.4 ± 10.2	41.9 ± 6.4	53.3 ± 21.7	88.1 ± 4.0	64.2 ± 7.9	35.6 ± 9.1
SO <sub>4</sub> <sup>2-</sup> /μg m <sup>-3</sup>	9.4 ± 3.3	12.5 ± 2.4	8.9 ± 2.1	6.0 ± 1.6	11.6 ± 4.7	15.8 ± 4.5	13.9 ± 3.6	8.9 ± 3.7
NO <sub>3</sub> <sup>-</sup> /μg m <sup>-3</sup>	17.4 ± 8.3	25.9 ± 5.5	15.5 ± 5.2	8.5 ± 1.3	14.8 ± 5.3	21.7 ± 2.9	16.3 ± 3.3	11.7 ± 4.6
NH <sub>4</sub> <sup>+</sup> /μg m <sup>-3</sup>	7.1 ± 3.0	9.9 ± 2.0	6.7 ± 1.8	3.6 ± 0.7	6.8 ± 2.7	9.3 ± 1.2	8.3 ± 1.7	5.0 ± 2.2
Cl <sup>-</sup> /μg m <sup>-3</sup>	2.1 ± 0.8	2.7 ± 0.6	2.2 ± 0.7	1.1 ± 0.3	1.7 ± 1.1	2.9 ± 0.9	1.8 ± 1.0	1.3 ± 0.9
K <sup>+</sup> /μg m <sup>-3</sup>	0.8 ± 0.3	1.0 ± 0.2	0.8 ± 0.2	0.6 ± 0.1	0.9 ± 0.5	1.5 ± 0.3	1.0 ± 0.4	0.6 ± 0.4
Ca <sup>2+</sup> /μg m <sup>-3</sup>	1.8 ± 0.7	1.8 ± 0.7	1.7 ± 0.8	1.9 ± 0.4	1.5 ± 0.8	1.9 ± 0.6	1.9 ± 0.8	1.1 ± 0.6
Mg <sup>2+</sup> /μg m <sup>-3</sup>	0.10 ± 0.07	0.10 ± 0.03	0.09 ± 0.02	0.14 ± 0.13	0.06 ± 0.02	0.08 ± 0.01	0.06 ± 0.01	0.06 ± 0.01
TC/μg m <sup>-3</sup>	15.2 ± 5.3	17.6 ± 5.0	15.5 ± 5.6	11.5 ± 3.4	15.2 ± 6.7	25.2 ± 4.8	18.1 ± 3.6	10.4 ± 3.5
NOR	0.22	0.27	0.21	0.14	0.26	0.32	0.26	0.23
SOR	0.49	0.48	0.43	0.34	0.57	0.65	0.65	0.59
NOR/SOR	0.45	0.56	0.49	0.41	0.46	0.49	0.40	0.39
NO <sub>3</sub> <sup>-</sup> /SO <sub>4</sub> <sup>2-</sup>	1.9	2.1	1.7	1.4	1.3	1.4	1.2	1.3
NO <sub>2</sub> /μg m <sup>-3</sup>	60.8	69.6	57.4	53.7	42.3	46.3	47.0	38.2
SO <sub>2</sub> /μg m <sup>-3</sup>	12.3	13.3	11.9	11.5	6.8	8.3	7.3	6.0

(b)								
	Guiyang (GY)				Kunming (KM)			
	Sampling Period	Polluted	Transition	Clean	Sampling Period	Polluted	Transition	Clean
PM <sub>2.5</sub> /μg m <sup>-3</sup>	39.4 ± 18.2	108.6	59.7 ± 7.9	32.6 ± 8.5	33.8 ± 11.2	—	63.0 ± 5.1	31.8 ± 8.3
SO <sub>4</sub> <sup>2-</sup> /μg m <sup>-3</sup>	11.3 ± 4.2	13.7	12.0 ± 3.7	11.1 ± 4.3	5.8 ± 3.3	—	13.2 ± 4.0	5.3 ± 2.6
NO <sub>3</sub> <sup>-</sup> /μg m <sup>-3</sup>	6.9 ± 5.1	6.2	11.0 ± 6.8	6.1 ± 4.5	2.8 ± 1.8	—	6.6 ± 0.2	2.5 ± 1.5
NH <sub>4</sub> <sup>+</sup> /μg m <sup>-3</sup>	5.4 ± 2.2	5.6	6.1 ± 2.4	5.3 ± 2.2	2.3 ± 1.4	—	5.2 ± 1.0	2.1 ± 1.2
Cl <sup>-</sup> /μg m <sup>-3</sup>	0.5 ± 0.2	0.7	0.6 ± 0.2	0.4 ± 0.2	0.8 ± 0.4	—	1.5 ± 0.5	0.7 ± 0.4
K <sup>+</sup> /μg m <sup>-3</sup>	0.5 ± 0.3	0.6	0.5 ± 0.3	0.4 ± 0.3	0.3 ± 0.1	—	0.5 ± 0.1	0.3 ± 0.1
Ca <sup>2+</sup> /μg m <sup>-3</sup>	2.5 ± 1.0	3.5	2.9 ± 1.4	2.4 ± 0.9	2.2 ± 0.9	—	2.6 ± 1.5	2.2 ± 0.8
Mg <sup>2+</sup> /μg m <sup>-3</sup>	0.08 ± 0.04	0.1	0.08 ± 0.02	0.08 ± 0.04	0.10 ± 0.03	—	0.09 ± 0.01	0.10 ± 0.03
TC/μg m <sup>-3</sup>	13.0 ± 6.2	16.6	14.7 ± 8.6	12.4 ± 5.8	12.0 ± 3.1	—	15.2 ± 2.3	11.8 ± 3.0
NOR	0.19	0.16	0.20	0.18	0.07	—	0.15	0.06
SOR	0.40	0.38	0.31	0.43	0.22	—	0.43	0.20
NOR/SOR	0.48	0.42	0.65	0.42	0.32	—	0.35	0.30
NO <sub>3</sub> <sup>-</sup> /SO <sub>4</sub> <sup>2-</sup>	0.6	0.5	0.9	0.6	0.5	—	0.5	0.5
NO <sub>2</sub> /μg m <sup>-3</sup>	30.1	33.3	44.0	27.2	37.2	—	38.1	37.2
SO <sub>2</sub> /μg m <sup>-3</sup>	17.2	22.5	27.2	15.0	20.8	—	17.8	21.0

Polluted: PM<sub>2.5</sub> > 80 μg m<sup>-3</sup>. Transition: 50 μg m<sup>-3</sup> ≤ PM<sub>2.5</sub> ≤ 80 μg m<sup>-3</sup>. Clean: PM<sub>2.5</sub> < 50 μg m<sup>-3</sup>.



**Figure 3.** Annual variations in winter PM<sub>2.5</sub> (a), SO<sub>4</sub><sup>2−</sup> (b), NO<sub>3</sub><sup>−</sup> (c), and NH<sub>4</sub><sup>+</sup> (d) concentrations in Chengdu and Chongqing (2010–2017).

### 3.2. Spatial–Temporal Variations in Water-Soluble Ionic Species

#### 3.2.1. Primary Chemical Species Leading to Polluted Days

The primary chemical species contributing to PM<sub>2.5</sub> mass, specifically sulfate (SO<sub>4</sub><sup>2−</sup>), nitrate (NO<sub>3</sub><sup>−</sup>), and ammonium (NH<sub>4</sub><sup>+</sup>), collectively known as SNA, along with total carbonaceous species (TC), constituted over 70% of the PM<sub>2.5</sub> composition across all sites. Detailed concentration distributions are presented in Table 1a,b and depicted in Figure 4. The mean concentrations of total SNA were 33.9, 33.2, 23.6, and 10.8 µg m<sup>−3</sup> at Chengdu (CD), Chongqing (CQ), Guiyang (GY), and Kunming (KM), respectively, contributing to 47.2%, 62.2%, 59.9%, and 32.0% of the total PM<sub>2.5</sub> mass. The specific contributions of SO<sub>4</sub><sup>2−</sup>, NO<sub>3</sub><sup>−</sup>, and NH<sub>4</sub><sup>+</sup> were notably different across these cities, reflecting varied pollution sources and atmospheric processing conditions.

In addition to SNA, TC was another significant contributor to PM<sub>2.5</sub>, accounting for 21.2%, 28.6%, 32.8%, and 35.6% of the particulate matter mass at CD, CQ, GY, and KM, respectively. The spatial and temporal variations in SNA and TC during different pollution episodes were complex. Notably, the ratios of SNA/PM<sub>2.5</sub> did not consistently align with those of PM<sub>2.5</sub> mass concentrations or TC/PM<sub>2.5</sub> ratios. For example, average SNA contributions to PM<sub>2.5</sub> varied from 43.3% to 48.6% in CD, whereas in CQ and GY, the range was significantly broader, from 53.2% to 72.0% and 23.5% to 68.9%, respectively.

During pollution episodes, the patterns of SNA/PM<sub>2.5</sub> ratios varied: they generally decreased on polluted days compared to clean days in CD, indicating a higher increase in other PM<sub>2.5</sub> components under polluted conditions, while the opposite trend was observed in CQ and GY, suggesting variable influencing factors on PM<sub>2.5</sub> composition in these regions. This variability in SNA and OC contributions on polluted days aligns with



findings from [31], indicating significant regional differences in source contributions and atmospheric conditions.

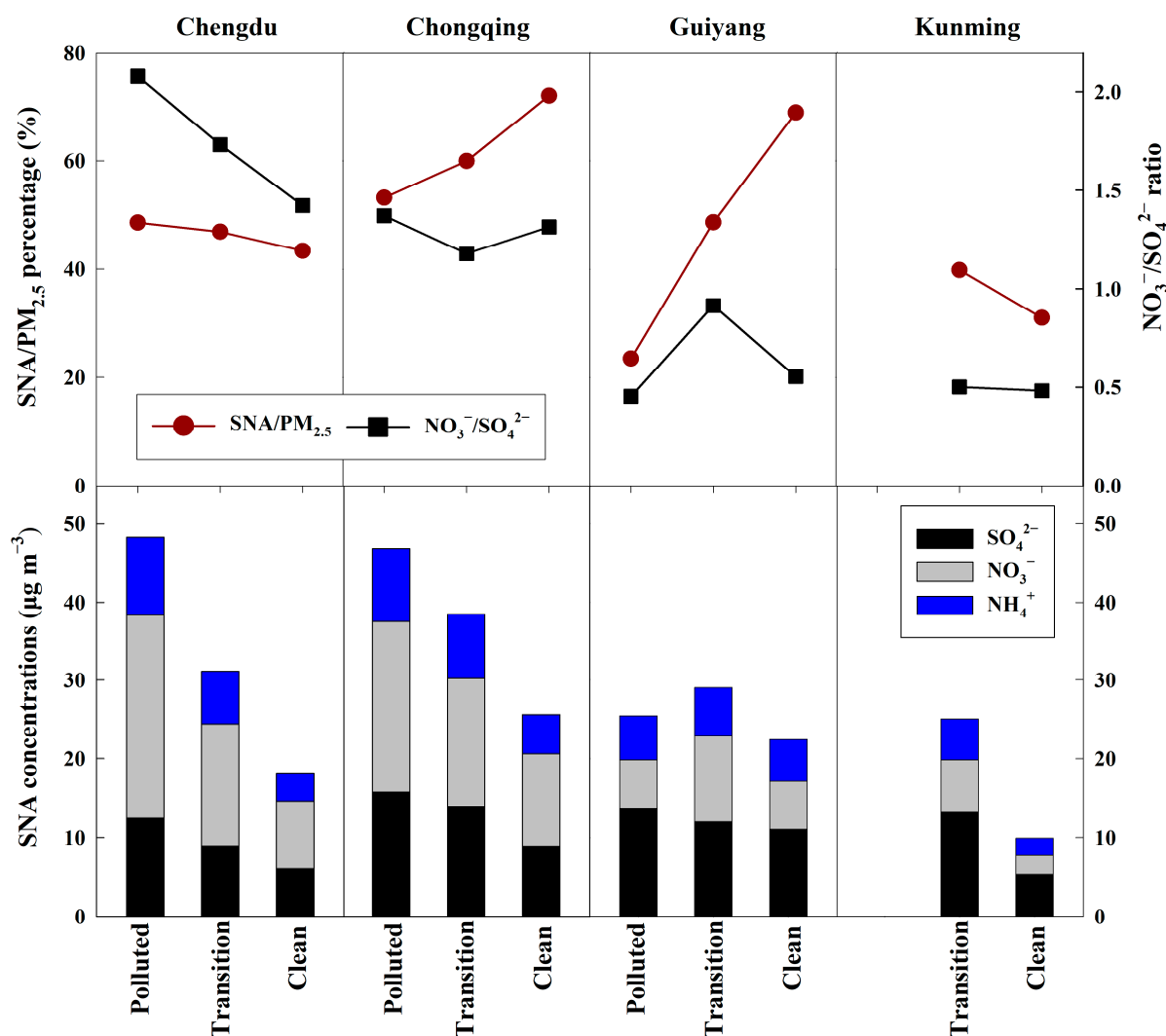


**Figure 4.** Variations in water-soluble ions  $\Sigma$ SNA ( $=\text{SO}_4^{2-} + \text{NO}_3^- + \text{NH}_4^+$ ),  $\text{NO}_3^-/\text{SO}_4^{2-}$  ratios, and  $\Sigma$ SNA/PM<sub>2.5</sub> mass percentages across different PM<sub>2.5</sub> concentration intervals (Polluted, Transition, Clean) for each study site.

The individual increases in SNA species on polluted days compared to clean days also varied (Figure 5). While NO<sub>3</sub><sup>-</sup> saw the highest increase, up to 3.1-fold in CD, SO<sub>4</sub><sup>2-</sup> had a more moderate increase, and NH<sub>4</sub><sup>+</sup> even decreased slightly in GY on polluted days. This points to the dynamic nature of aerosol chemistry under different atmospheric conditions.

Furthermore, potassium (K<sup>+</sup>) and chloride (Cl<sup>-</sup>) concentrations were particularly elevated on polluted days, especially in CQ, often linked to biomass burning and possibly coal combustion in this region [28,42,58]. Unlike K<sup>+</sup> and Cl<sup>-</sup>, calcium (Ca<sup>2+</sup>) concentrations, often indicative of construction dust, showed notable increases on polluted days in GY and KM, reflecting ongoing urban development and insufficient dust control measures in these areas [17,59].

These detailed analyses of water-soluble ions and carbonaceous species in PM<sub>2.5</sub> provide crucial insights into the sources and processes affecting air quality in southwestern China, highlighting the need for targeted pollution control strategies tailored to specific regional conditions.

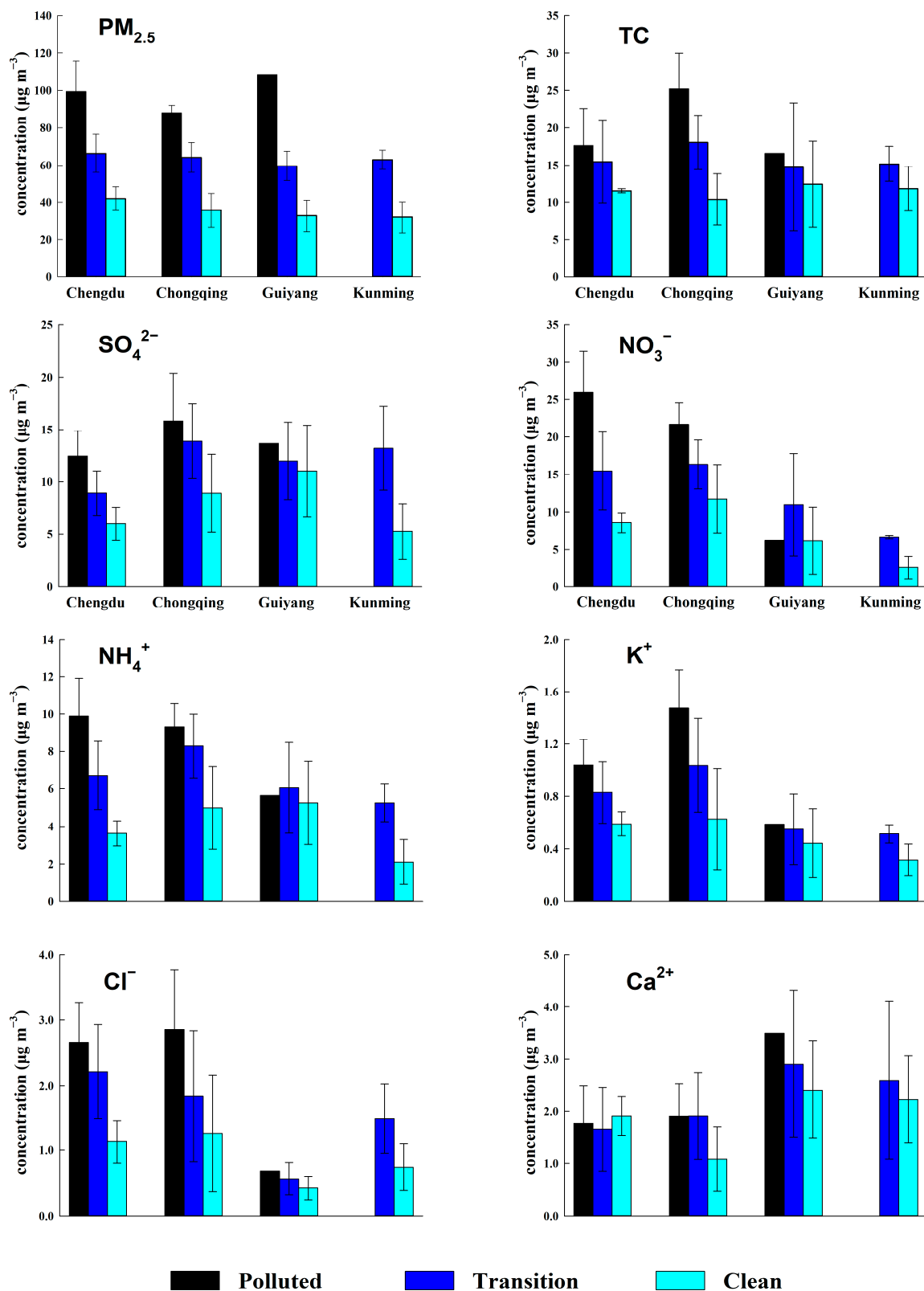


**Figure 5.** Individual water-soluble ion concentrations across different PM<sub>2.5</sub> concentration intervals (Polluted, Transition, Clean).

### 3.2.2. Importance and Mechanisms of Nitrate and Sulfate Formation

The emissions of sulfur dioxide (SO<sub>2</sub>) predominantly originate from coal combustion, while nitrogen oxides (NO<sub>x</sub>) are primarily emitted from vehicular exhausts in urban envi-

ronments [60]. Sulfate and nitrate are formed through photochemical reactions involving these gaseous precursors [61]. Prior research has shown that the  $\text{NO}_3^-/\text{SO}_4^{2-}$  ratio can be used to effectively gauge the relative contributions of mobile and stationary sources to atmospheric sulfur and nitrogen in China [25,62,63]. In this study, the  $\text{NO}_3^-/\text{SO}_4^{2-}$  ratios ranged from 0.48 to 2.08. Spatial analysis revealed that the average  $\text{NO}_3^-/\text{SO}_4^{2-}$  values were ordered as follows: Chengdu (CD) (1.84) > Chongqing (CQ) (1.27) > Guiyang (GY) (0.61) > Kunming (KM) (0.48). Compared to other cities, Chengdu's ratio was notably higher than Beijing (0.71) and Shanghai (0.64), where traffic density is significant, and only surpassed by Guangzhou (2.14), a city with minimal coal combustion [27,64,65].

Temporal analysis showed a consistent increase in the  $\text{NO}_3^-/\text{SO}_4^{2-}$  ratio from clean to polluted days in Chengdu, suggesting a significant role for nitrate formation in the city's haze pollution. In contrast, fluctuations in this ratio were minimal in the other cities, indicating a stable source pattern. This trend suggests that, in Chengdu, mobile sources have become the predominant contributor to  $\text{PM}_{2.5}$ , overshadowing stationary sources. Despite the growing impact of vehicular emissions, the contribution of stationary sources remains significant in the other cities.

Meteorological and chemical conditions in Chengdu appear more favorable for nitrate formation compared to Chongqing and elsewhere. Furthermore, the sulfur oxidation ratio (SOR) and nitrogen oxidation ratio (NOR), used to evaluate the degree of secondary transformation, generally indicated extensive secondary photochemical oxidation of  $\text{SO}_2$  and  $\text{NO}_2$  when exceeding 0.10 [54,63,66]. In all sites, SOR values exceeded 0.10 across various pollution levels, highlighting the presence of secondary sulfate ions. The highest SOR was observed on polluted days in CQ (0.65), with the lowest on transformation days in GY (0.31), showing a mild increasing trend with pollution levels. This pattern is likely due to the elevated relative humidity in the Sichuan Basin during winter, which significantly promotes the secondary formation of sulfate [28,54].

NOR values were generally lower than SOR, with the highest NOR observed in CQ (0.32) on polluted days and the lowest in KM (0.06) on clean days. The NOR/SOR ratio's variation with pollution levels suggests that  $\text{NO}_2$  transformation becomes more significant under heavy pollution, especially in CD and CQ. Over a longer time scale, from 2010 to 2017, a consistent trend was observed during the winter months. As depicted in Figure 3, the concentrations of sulfate and  $\text{PM}_{2.5}$  show a consistent decline over the years (Figure 3b), while nitrate ions exhibit the opposite trend, increasing annually (Figure 3c). The ammonium ion content remains relatively stable, showing minimal variation (Figure 3d). These trends suggest that nitrate formation is increasingly playing a pivotal role in the region's haze dynamics, corroborating findings from recent studies by [60,61], which highlight the growing appearance of nitrate in the urban haze under changing atmospheric conditions. Given that ammonium concentrations remain stable, it is advantageous to implement targeted monitoring programs focusing on reducing emissions from agricultural and industrial sources contributing to these levels. Such programs can help mitigate the impact of ammonium on  $\text{PM}_{2.5}$  pollution, contributing to overall air quality improvement. This targeted approach aligns with the need for specific interventions to address stable pollutant levels and their sources effectively.

### 3.3. $\text{PM}_{2.5}$ Source Apportionment

Utilizing the EPA PMF 5.0 model, this study analyzed  $\text{PM}_{2.5}$  concentration data across four urban sites, with inputs comprising arithmetic mean values and standard deviations. The analysis identified six key sources of  $\text{PM}_{2.5}$ : coal combustion, vehicle emissions, secondary inorganic sulfate (SIS), secondary inorganic nitrate (SIN), construction dust, and biomass burning, detailed in Figure 6.

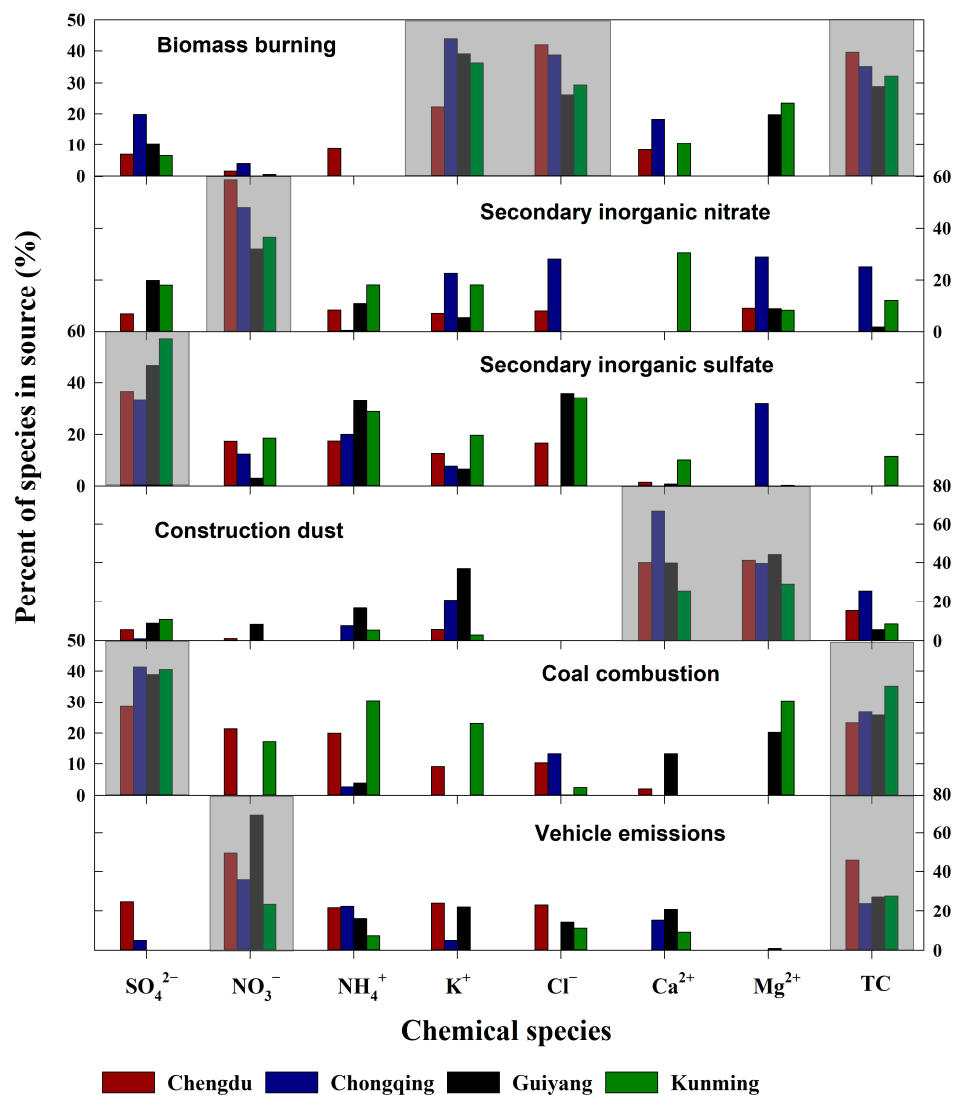


**Figure 6.** Factor profiles resolved from the PMF model for atmospheric PM<sub>2.5</sub> at four urban sites (shaded sections indicate the key chemical markers that identify each source).

Biomass burning, the first identified source, is marked by elevated K<sup>+</sup> levels, a known tracer for biomass combustion aerosols [17,67]. While high Cl<sup>-</sup> levels are sometimes linked to marine sources, within China's interior, they more likely originate from coal or biomass burning [58,68]. SIN and SIS are distinguished by their NO<sub>3</sub><sup>-</sup> and SO<sub>4</sub><sup>2-</sup> markers, respectively. Construction dust, identified through elevated Ca<sup>2+</sup> and Mg<sup>2+</sup>, includes both fugitive and resuspended road dust, with calcium serving as a principal indicator for such dust in urban centers [17,59,69]. Coal combustion, associated with SO<sub>4</sub><sup>2-</sup> and total carbon (TC), remains the primary energy source, notably in China's less-developed southwestern regions, where it has historically contributed to acid rain [70]. Previous studies also identify coal combustion as a significant source of TC [71,72]. The last identified source, vehicle emissions, is characterized by NO<sub>3</sub><sup>-</sup> and TC, compounds typically enriched in vehicular exhaust fumes [73,74].

Figure 7 delineates the proportional contributions of each source to PM<sub>2.5</sub> concentrations across the four cities. In Chengdu, vehicle emissions dominate, contributing 33.1% to PM<sub>2.5</sub> mass, followed by SIS and SIN (25.5%), coal combustion (20.3%), biomass burning (15.7%), and construction dust (5.4%). Chongqing's profile shows SIS and SIN as the leading contributors (36%), closely followed by coal combustion and vehicle emissions. In contrast, Guiyang's PM<sub>2.5</sub> burden is predominantly from coal combustion (46.3%), with vehicle emissions also significant (32.7%). Kunming presents a more distributed source profile,

with coal combustion leading, followed by vehicle emissions and secondary aerosols. These results of the PMF analysis are consistent with the daily average variations in  $PM_{2.5}$  loading and its SNA (Figure 4) and with the ions presented above (Figure 5).

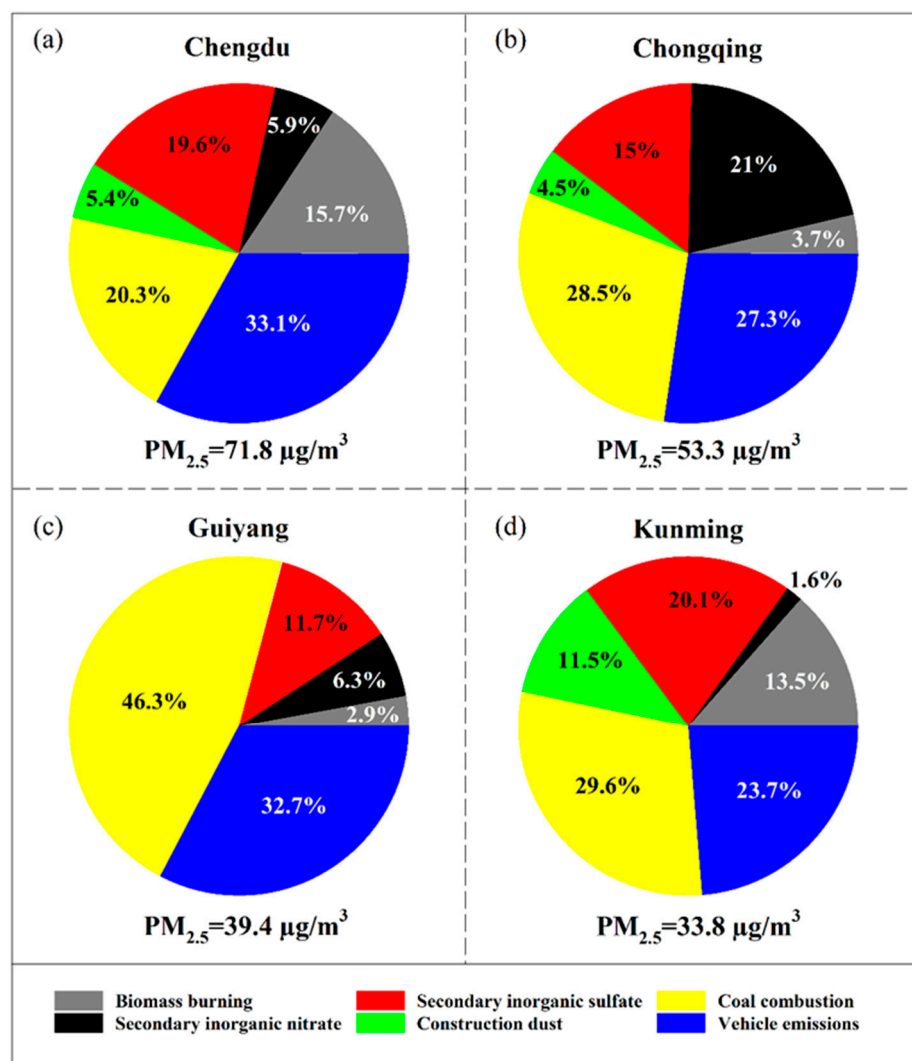


**Figure 7.** Positive matrix factorization (PMF) resolved source contributions to  $PM_{2.5}$  at four urban sites (a–d represent Chengdu, Chongqing, Guiyang, and Kunming respectively).

In summary, Chengdu and Chongqing exhibit a high influence of vehicle emissions and secondary inorganic aerosols on  $PM_{2.5}$  concentrations, indicative of the significant role of transportation and industrial activities in these urban areas. In Guiyang, coal combustion emerges as the predominant source of  $PM_{2.5}$ , underscoring the city's reliance on coal for energy and the associated air quality challenges. Kunming's data reveal a more balanced distribution among sources, with coal combustion still leading but followed closely by vehicle emissions and secondary inorganic aerosols, suggesting a mix of industrial, vehicular, and natural sources contributing to the  $PM_{2.5}$  burden. These source profiles for the four urban sampling sites are consistent with the results of several earlier studies. For instance, compared to ten years ago,  $SO_4^{2-}$  concentrations are reduced while  $NO_3^-$  levels are elevated, probably due to the greater vehicle-using population in the Sichuan Basin [28].

### 3.4. Backward Trajectory Analysis

The backward trajectory analysis, a tool for tracing the origins and pathways of air masses, was employed for the four study sites, offering insights into the regional and



long-distance transport of pollutants [16]. As illustrated in Figure 8, the trajectories were categorized into five distinct types based on their origins and paths. For Chengdu, clusters 1 and 4, representing 76.7% of the air masses, were predominantly local, originating within Sichuan Province. The remaining 23.3% (clusters 2, 3, and 5) were traced back to western China and India, highlighting a mix of regional and long-distance influences on Chengdu's air quality (Figure 8a). Chongqing's air mass analysis revealed a significant portion (43.3%) of local origin (cluster 4), with cluster 1 (26.7%) coming from Hubei. Clusters 2 and 3, which accounted for 23.3%, followed a path from India through Nepal, Bangladesh, and Myanmar, demonstrating the impact of long-distance air transport, particularly in winter. This pattern aligns with findings from several studies indicating that air pollutants from India can reach southwestern Chinese cities via prevailing westerlies [30,75,76]. Cluster 5, making up 6.7%, originated from Qinghai (Figure 8b). Guiyang showed more diversified trajectory origins, with trajectories 1, 2, 3, 4, and 5 contributing to 50%, 20%, 20%, 6.7%, and 3.3% of the total trajectories, respectively. The majority were local (trajectory 1 from Guizhou) or from neighboring regions like Hubei, Chongqing, Burma, and Zhejiang (Figure 8c). Kunming's analysis pointed to a dominance of local air masses (trajectories 1 and 2 accounting for 76.7%), originating from Yunnan's own locale, underscoring the significant local contributions to the city's air mass during winter (Figure 8d). To further enhance the robustness and transparency of air quality monitoring, integrating advanced technologies such as blockchain-based systems is recommended. These systems can ensure data integrity and improve the reliability of air pollution measurements, providing real-time, tamper-proof monitoring data. Sofia et al. [77] outline a promising approach that could be particularly valuable in addressing the challenges of ensuring accurate and transparent data collection and reporting. Incorporating such innovative technologies could significantly enhance the effectiveness of air quality management strategies in southwestern China, ultimately contributing to more informed decision-making and policy development.

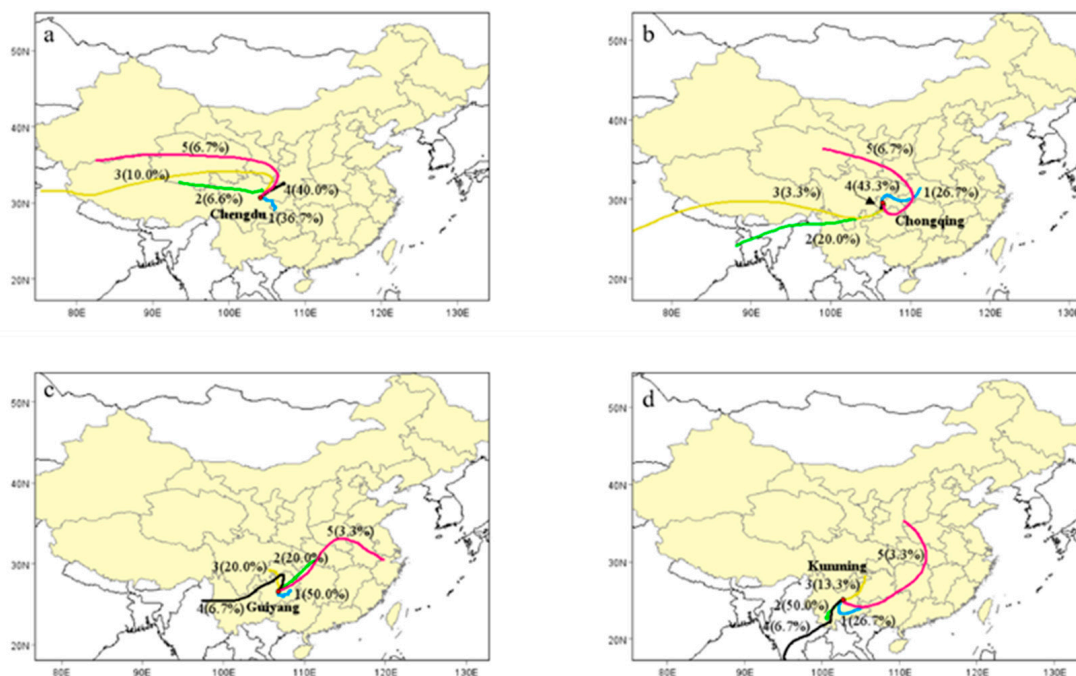


**Figure 8.** Backward trajectory clustering results for sampling periods. (a–d) represent Chengdu, Chongqing, Guiyang, and Kunming, respectively (different colors show the trajectories and the proportions of air masses expressed as percentages).

In summary, the backward trajectory analysis across the four cities during winter underscored the predominance of local air masses in shaping air quality. However, it also

highlighted the significant role of long-distance transport, particularly from India and adjacent provinces, in influencing the air mass composition. This dual influence underscores the complexity of air pollution dynamics, necessitating comprehensive strategies that address both local and transboundary pollution sources.

#### 4. Conclusions

This study rigorously examined PM<sub>2.5</sub> concentrations across Chengdu, Chongqing, Guiyang, and Kunming during the 2017 winter haze period, unveiling significant spatial-temporal variations. In Chengdu, PM<sub>2.5</sub> levels were more than twice the China Class II air quality standard of 35 µg m<sup>-3</sup>, with average concentrations reaching 71.8 ± 25.8 µg m<sup>-3</sup>. Similarly, Chongqing and Guiyang exceeded this standard, highlighting severe air quality issues exacerbated by urban and industrial activities. In contrast, Kunming maintained levels below this threshold, illustrating less severe pollution. Chemical composition analysis showed that water-soluble ions—sulfate, nitrate, and ammonium—alongside total carbonaceous species contributed over 70% to the PM<sub>2.5</sub> mass across all examined locations, indicating significant secondary formation processes alongside primary emissions.

Source apportionment efforts identified that vehicle emissions and secondary inorganic aerosols were the leading contributors in the heavily urbanized areas of Chengdu and Chongqing. In Guiyang, coal combustion was the predominant source, reflecting its reliance on coal for energy. This variance underscores the regional differences in industrial activities and their impacts on air quality. Furthermore, backward trajectory analysis emphasized the dual influence on pollution levels, with local emissions being the primary contributors, complemented by significant long-distance transport effects, particularly from India, during the winter season.

The interplay of local emission sources, regional industrial activities, and meteorological conditions underscores the complexity of managing PM<sub>2.5</sub> pollution. To effectively tackle these challenges, a multifaceted approach involving stricter emission regulations, regional collaboration for air quality management, and robust monitoring systems is essential. Promoting regional collaboration between cities in southwestern China and neighboring regions is essential for addressing transboundary pollution. Creating a shared air monitoring network and developing joint mitigation strategies can improve the effectiveness of regional interventions, fostering a collaborative approach to air quality management. Such efforts will facilitate the sharing of data, resources, and best practices, ultimately leading to more effective and coordinated pollution control measures. Additionally, investing in advanced emission control technologies in the industrial and transportation sectors can lead to significant improvements in air quality. Adopting filtration technologies and catalysts to reduce particulate emissions from vehicles and industries is a promising strategy that should be pursued urgently. These advanced technologies can help mitigate the impact of these sectors on PM<sub>2.5</sub> pollution, contributing to cleaner air and better public health outcomes.

**Author Contributions:** H.G.: writing—original draft, investigation, funding acquisition, formal analysis, data curation, conceptualization, project administration. Z.C.: investigation, data curation. J.T.: validation, investigation. H.X.: supervision, investigation. All authors have read and agreed to the published version of the manuscript.

**Funding:** This research was funded by the Guizhou Provincial Science and Technology Projects (Grant NO. ZK[2021]212).

**Institutional Review Board Statement:** Not applicable.

**Informed Consent Statement:** Not applicable.

**Data Availability Statement:** Data available on request due to restrictions privacy. The data presented in this study are available on request from the corresponding author.

**Conflicts of Interest:** The authors declare no conflicts of interest.

## References

1. Pope, C.A.; Dockery, D.W. Health effects of fine particulate air pollution: Lines that connect. *J. Air Waste Manag. Assoc.* **2006**, *56*, 709–742. [[CrossRef](#)] [[PubMed](#)]
2. Anderson, G.B.; Krall, J.R.; Peng, R.D.; Bell, M.L. Is the Relation Between Ozone and Mortality Confounded by Chemical Components of Particulate Matter? Analysis of 7 Components in 57 US Communities. *Am. J. Epidemiol.* **2012**, *176*, 726–732. [[CrossRef](#)] [[PubMed](#)]
3. Lepeule, J.; Laden, F.; Dockery, D.; Schwartz, J. Chronic Exposure to Fine Particles and Mortality: An Extended Follow-up of the Harvard Six Cities Study from 1974 to 2009. *Environ. Health Perspect.* **2012**, *120*, 965–970. [[CrossRef](#)] [[PubMed](#)]
4. Wen, L.; Yang, C.; Liao, X.; Zhang, Y.; Chai, X.; Gao, W.; Guo, S.; Bi, Y.; Tsang, S.Y.; Chen, Z.F.; et al. Investigation of PM<sub>2.5</sub> pollution during COVID-19 pandemic in Guangzhou, China. *J. Environ. Sci.* **2022**, *115*, 443–452. [[CrossRef](#)] [[PubMed](#)]
5. Cao, J.J.; Wang, Q.Y.; Chow, J.C.; Watson, J.G.; Tie, X.; Shen, Z.; Wang, P.; An, Z. Impacts of aerosol compositions on visibility impairment in Xi'an, China. *Atmos. Environ.* **2012**, *59*, 559–566. [[CrossRef](#)]
6. Fu, X.; Wang, X.; Hu, Q.; Li, G.; Ding, X.; Zhang, Y.; He, Q.; Liu, T.; Zhang, Z.; Yu, Q.; et al. Changes in visibility with PM<sub>2.5</sub> composition and relative humidity at a background site in the Pearl River Delta region. *J. Environ. Sci.* **2016**, *40*, 10–19. [[CrossRef](#)] [[PubMed](#)]
7. Yang, N.; Shi, H.; Tang, H.; Yang, X. Geographical and temporal encoding for improving the estimation of PM<sub>2.5</sub> concentrations in China using end-to-end gradient boosting. *Remote Sens. Environ.* **2022**, *269*, 112828. [[CrossRef](#)]
8. Jacob, D.J.; Winner, D.A. Effect of climate change on air quality. *Atmos. Environ.* **2009**, *43*, 51–63. [[CrossRef](#)]
9. Mahowald, N. Aerosol Indirect Effect on Biogeochemical Cycles and Climate. *Science* **2011**, *334*, 794–796. [[CrossRef](#)] [[PubMed](#)]
10. Huang, R.J.; Zhang, Y.; Bozzetti, C.; Ho, K.F.; Cao, J.J.; Han, Y.; Daellenbach, K.R.; Slowik, J.G.; Platt, S.M.; Canonaco, F.; et al. High secondary aerosol contribution to particulate pollution during haze events in China. *Nature* **2014**, *514*, 218–222. [[CrossRef](#)]
11. Lu, P.; Deng, S.; Li, G.; Li, J.; Xu, K.; Lu, Z. Spatial distribution of primary and secondary PM<sub>2.5</sub> concentrations emitted by vehicles in the Guanzhong Plain, China. *Atmosphere* **2022**, *13*, 347. [[CrossRef](#)]
12. Wei, F.; Teng, E.; Wu, G.; Hu, W.; Wilson, W.E.; Chapman, R.S.; Pau, J.C.; Zhang, J. Ambient concentrations and elemental compositions of PM<sub>10</sub> and PM<sub>2.5</sub> in four Chinese cities. *Environ. Sci. Technol.* **1999**, *33*, 4188–4193. [[CrossRef](#)]
13. Huang, X.F.; He, L.Y.; Hu, M.; Zhang, Y.H. Annual variation of particulate organic compounds in PM<sub>2.5</sub> in the urban atmosphere of Beijing. *Atmos. Environ.* **2006**, *40*, 2449–2458. [[CrossRef](#)]
14. Tiwari, S.; Srivastava, A.K.; Bisht, D.S.; Bano, T.; Singh, S.; Behura, S.; Srivastava, M.K.; Chate, D.M.; Padmanabhamurty, B. Black carbon and chemical characteristics of PM<sub>10</sub> and PM<sub>2.5</sub> at an urban site of North India. *J. Atmos. Chem.* **2009**, *62*, 193–209. [[CrossRef](#)]
15. Tao, J.; Cheng, T.; Zhang, R.; Cao, J.; Zhu, L.; Wang, Q.; Luo, L.; Zhang, L.M. Chemical composition of PM<sub>2.5</sub> at an urban site of Chengdu in southwestern China. *Adv. Atmos. Sci.* **2013**, *30*, 1070–1084. [[CrossRef](#)]
16. Zhang, T.; Cao, J.J.; Chow, J.C.; Shen, Z.X.; Ho, K.F.; Ho, S.S.H.; Liu, S.X.; Han, Y.M.; Waston, J.G.; Wang, G.H.; et al. Characterization and seasonal variations of levoglucosan in fine particulate matter in Xi'an, China. *J. Air Waste Manag. Assoc.* **2014**, *64*, 1317–1327. [[CrossRef](#)] [[PubMed](#)]
17. Wang, G.; Cheng, S.; Li, J.; Lang, J.; Wen, W.; Yang, X.; Tian, L. Source apportionment and seasonal variation of PM<sub>2.5</sub> carbonaceous aerosol in the Beijing-Tianjin-Hebei Region of China. *Environ. Monit. Assess.* **2015**, *187*, 143. [[CrossRef](#)] [[PubMed](#)]
18. Lyu, X.; Chen, N.; Guo, H.; Zeng, L.; Zhang, W.; Shen, F.; Quan, J.H.; Wang, N. Chemical characteristics and causes of airborne particulate pollution in warm seasons in Wuhan, Central China. *Atmos. Chem. Phys.* **2016**, *16*, 10671–10687. [[CrossRef](#)]
19. Wang, J.; Zhao, B.; Wang, S.; Yang, F.; Xing, J.; Morawska, L.; Ding, A.J.; Kulmala, M.; Kerminen, V.M.; Kujansuu, J.; et al. Particulate matter pollution over China and the effects of control policies. *Sci. Total Environ.* **2017**, *584*, 426–447. [[CrossRef](#)] [[PubMed](#)]
20. Lai, S.C.; Zou, S.C.; Cao, J.J.; Lee, S.C.; Ho, K.F. Characterizing ionic species in PM<sub>2.5</sub> and PM<sub>10</sub> in four Pearl River Delta cities, South China. *J. Environ. Sci.* **2007**, *19*, 939–947. [[CrossRef](#)] [[PubMed](#)]
21. Meng, Z.Y.; Zhang, R.J.; Lin, W.L.; Jia, X.F.; Yu, X.M.; Yu, X.L.; Wang, G.H. Seasonal variation of ammonia and ammonium aerosol at a background station in the Yangtze River Delta Region, China. *Aerosol Air Qual. Res.* **2014**, *14*, 756–766. [[CrossRef](#)]
22. Han, L.; Cheng, S.; Zhuang, G.; Ning, H.; Wang, H.; Wei, W.; Zhao, X. The changes and long-range transport of PM<sub>2.5</sub> in Beijing in the past decade. *Atmos. Environ.* **2015**, *110*, 186–195. [[CrossRef](#)]
23. Ji, D.; Zhang, J.; He, J.; Wang, X.; Pang, B.; Liu, Z.; Wang, L.L.; Wang, Y.S. Characteristics of atmospheric organic and elemental carbon aerosols in urban Beijing, China. *Atmos. Environ.* **2016**, *125*, 293–306. [[CrossRef](#)]
24. Tan, J.; Duan, J.; Ma, Y.; He, K.; Cheng, Y.; Deng, S.X.; Huang, Y.L.; Si-Tu, S.P. Long-term trends of chemical characteristics and sources of fine particle in Foshan City, Pearl River Delta: 2008–2014. *Sci. Total Environ.* **2016**, *565*, 519–528. [[CrossRef](#)]
25. Liu, P.; Zhang, C.; Xue, C.; Mu, Y.; Liu, J.; Zhang, Y.; Tian, D.; Ye, C.; Zhang, H.; Guan, J. The contribution of residential coal combustion to atmospheric PM<sub>2.5</sub> in northern China during winter. *Atmos. Chem. Phys.* **2017**, *17*, 11503–11520. [[CrossRef](#)]
26. Li, J.; Liao, H.; Hu, J.; Li, N. Severe particulate pollution days in China during 2013–2018 and the associated typical weather patterns in Beijing-Tianjin-Hebei and the Yangtze River Delta regions. *Environ. Pollut.* **2019**, *248*, 74–81. [[CrossRef](#)] [[PubMed](#)]
27. Yang, F.; Tan, J.; Zhao, Q.; Du, Z.; He, K.; Ma, Y.; Duan, F.; Chen, G.; Zhao, Q. Characteristics of PM<sub>2.5</sub> speciation in representative megacities and across China. *Atmos. Chem. Phys.* **2011**, *11*, 5207–5219. [[CrossRef](#)]

28. Tian, M.; Wang, H.; Chen, Y.; Zhang, L.; Shi, G.; Liu, Y.; Yu, J.; Zhai, C.; Wang, J.; Yang, F. Highly time-resolved characterization of water-soluble inorganic ions in PM<sub>2.5</sub> in a humid and acidic mega city in Sichuan Basin, China. *Sci. Total Environ.* **2017**, *580*, 224–234. [[CrossRef](#)] [[PubMed](#)]
29. Xiao, H.Y.; Liu, C.Q. Sources of nitrogen and sulfur in wet deposition at Guiyang, southwest China. *Atmos. Environ.* **2002**, *36*, 5121–5130. [[CrossRef](#)]
30. Li, L.; Tan, Q.; Zhang, Y.; Feng, M.; Qu, Y.; An, J.; Liu, X. Characteristics and source apportionment of PM<sub>2.5</sub> during persistent extreme haze events in Chengdu, southwest China. *Environ. Pollut.* **2017**, *230*, 718–729. [[CrossRef](#)] [[PubMed](#)]
31. Wang, H.; Tian, M.; Chen, Y.; Shi, G.; Liu, Y.; Yang, F.; Zhang, L.; Deng, L.; Yu, J.; Peng, C.; et al. Seasonal characteristics, formation mechanisms and source origins of PM<sub>2.5</sub> in two megacities in Sichuan Basin, China. *Atmos. Chem. Phys.* **2018**, *18*, 865–881. [[CrossRef](#)]
32. Kong, L.; Tan, Q.; Feng, M.; Qu, Y.; An, J.; Liu, X.; Cheng, N.; Deng, Y.; Zhai, R.; Wang, Z. Investigating the characteristics and source analyses of PM<sub>2.5</sub> seasonal variations in Chengdu, Southwest China. *Chemosphere* **2020**, *243*, 125267. [[CrossRef](#)] [[PubMed](#)]
33. Xiao, H.; Xiao, H.Y.; Zhang, Z.Y.; Zheng, N.J.; Li, Q.K.; Li, X.D. Chemical characteristics of major inorganic ions in PM<sub>2.5</sub> based on year-long observations in Guiyang, Southwest China-implications for formation pathways and the influences of regional transport. *Atmosphere* **2020**, *11*, 847. [[CrossRef](#)]
34. Yang, X.; Lu, Y.; Zhu, X.; He, J.; Jiang, Q.; Wu, K.; Wang, H.; Zhang, X.; Wang, S. Formation and evolution mechanisms of severe haze pollution in the Sichuan basin, southwest China. *Aerosol Air Qual. Res.* **2020**, *20*, 2557–2567. [[CrossRef](#)]
35. Liu, Y.; Shi, G.; Zhan, Y.; Zhou, L.; Yang, F. Characteristics of PM<sub>2.5</sub> spatial distribution and influencing meteorological conditions in Sichuan Basin, southwestern China. *Atmos. Environ.* **2021**, *253*, 118364. [[CrossRef](#)]
36. Ali, M.A.; Huang, Z.; Bilal, M.; Assiri, M.E.; Mhawish, A.; Nichol, J.E.; Leeuw, G.; Almazroui, M.; Wang, Y.; Alsubhi, Y. Long-term PM<sub>2.5</sub> pollution over China: Identification of PM<sub>2.5</sub> pollution hotspots and source contributions. *Sci. Total Environ.* **2023**, *893*, 164871. [[CrossRef](#)] [[PubMed](#)]
37. Chan, C.K.; Yao, X.H. Review: Air pollution in mega cities in China. *Atmos. Environ.* **2008**, *42*, 1–42. [[CrossRef](#)]
38. Liu, X.Y.; Xiao, H.Y.; Liu, C.Q.; Xiao, H.W.; Wang, Y.L. Assessment of atmospheric sulfur with the epilithic moss *Haplodadium microphyllum*: Evidences from tissue sulfur and  $\delta^{34}\text{S}$  analysis. *Environ. Pollut.* **2009**, *157*, 2066–2071. [[CrossRef](#)] [[PubMed](#)]
39. He, K.; Zhao, Q.; Ma, Y.; Duan, F.; Yang, F.; Shi, Z.; Chen, G. Spatial and seasonal variability of PM<sub>2.5</sub> acidity at two Chinese megacities: Insights into the formation of secondary inorganic aerosols. *Atmos. Chem. Phys.* **2012**, *12*, 1377–1395. [[CrossRef](#)]
40. Tian, M.; Liu, Y.; Yang, F.; Zhang, L.; Peng, C.; Chen, Y.; Shi, G.; Wang, H.; Luo, B.; Jiang, C.; et al. Increasing importance of nitrate formation for heavy aerosol pollution in two megacities in Sichuan Basin, southwest China. *Environ. Pollut.* **2019**, *250*, 898–905. [[CrossRef](#)] [[PubMed](#)]
41. Zhang, B.; Wang, S.; Wang, D.; Wang, Q.; Yang, X.; Tong, R. Air quality changes in China 2013–2020: Effectiveness of clean coal technology policies. *J. Clean. Prod.* **2022**, *366*, 132961. [[CrossRef](#)]
42. Shen, Z.X.; Cao, J.J.; Arimoto, R.; Han, Z.W.; Zhang, R.J.; Han, Y.M.; Liu, S.X.; Okuda, T.; Nakao, S.; Tanka, S. Ionic composition of TSP and PM<sub>2.5</sub> during dust storms and air pollution episodes at Xi'an, China. *Atmos. Environ.* **2009**, *43*, 2911–2918. [[CrossRef](#)]
43. Zhang, T.; Cao, J.J.; Tie, X.X.; Shen, Z.X.; Liu, S.X.; Ding, H.; Han, Y.M.; Wang, G.H.; Ho, K.F.; Qiang, J.; et al. Water-soluble ions in atmospheric aerosols measured in Xi'an, China: Seasonal variations and sources. *Atmos. Res.* **2011**, *102*, 110–119. [[CrossRef](#)]
44. Wang, Y.Q.; Zhang, X.Y.; Draxler, R.R. TrajStat: GIS-based software that uses various trajectory statistical analysis methods to identify potential sources from long-term air pollution measurement data. *Environ. Model. Softw.* **2009**, *24*, 938–939. [[CrossRef](#)]
45. Stohl, A. Computation, accuracy and applications of trajectories-A review and bibliography. *Atmos. Environ.* **1998**, *32*, 947–966. [[CrossRef](#)]
46. Srivastava, D.; Xu, J.; Vu, T.V.; Liu, D.; Li, L.; Fu, P.; Hou, S.; Palmerola, N.M.; Shi, Z.; Harrison, R.M. Insight into PM<sub>2.5</sub> sources by applying positive matrix factorization (PMF) at an urban and rural site of Beijing. *Atmos. Chem. Phys. Discuss.* **2021**, *21*, 14703–14724. [[CrossRef](#)]
47. Zhang, Y.J.; Tang, L.L.; Wang, Z.; Yu, H.X.; Sun, Y.L.; Liu, D.; Qin, W.; Canonaco, F.; Prévôt, A.S.H.; Zhang, H.L.; et al. Insights into characteristics, sources, and evolution of submicron aerosols during harvest seasons in the Yangtze River delta region, China. *Atmos. Chem. Phys.* **2015**, *15*, 1331–1349. [[CrossRef](#)]
48. Zhang, Y.X.; Sheesley, R.J.; Schauer, J.J.; Lewandowski, M.; Jaoui, M.; Offenberg, J.H.; Kleindienst, T.E.; Edney, E.O. Source apportionment of primary and secondary organic aerosols using positive matrix factorization (PMF) of molecular markers. *Atmos. Environ.* **2009**, *43*, 5567–5574. [[CrossRef](#)]
49. GB 3095-2012; Ambient Air Quality Standards. Ministry of Environmental Protection of the People's Republic of China: Beijing, China, 2012.
50. Jia, Z.; Ordóñez, C.; Doherty, R.M.; Wild, O.; Turnock, S.T.; O'Connor, F.M. Modulation of daily PM<sub>2.5</sub> concentrations over China in winter by large-scale circulation and climate change. *Atmos. Chem. Phys.* **2023**, *23*, 2829–2842. [[CrossRef](#)]
51. Feng, W.; Wang, M.; Zhang, Y.; Dai, X.; Liu, X.; Xu, Y. Intraseasonal variation and future projection of atmospheric diffusion conditions conducive to extreme haze formation over eastern China. *Atmos. Ocean Sci. Lett.* **2020**, *13*, 346–355. [[CrossRef](#)]
52. Glavas, S.D.; Nikolakis, P.; Ambatzoglou, D.; Mihalopoulos, N. Factors affecting the seasonal variation of mass and ionic composition of PM<sub>2.5</sub> at a central Mediterranean coastal site. *Atmos. Environ.* **2008**, *42*, 5365–5373. [[CrossRef](#)]
53. Harrison, R.M.; Yin, J. Chemical speciation of PM<sub>2.5</sub> particles at urban background and rural sites in the UK atmosphere. *J. Environ. Monit.* **2010**, *12*, 1404–1414. [[CrossRef](#)] [[PubMed](#)]



54. Chen, Y.; Xie, S.D.; Luo, B.; Zhai, C. Characteristics and sources of water-soluble ions in PM<sub>2.5</sub> in the Sichuan Basin, China. *Atmosphere* **2019**, *10*, 78. [[CrossRef](#)]
55. Du, X.X.; Shi, G.M.; Zhao, T.L.; Yang, F.M.; Zheng, X.B.; Zhang, Y.J.; Tan, Q.W. Contribution of secondary particles to wintertime PM<sub>2.5</sub> during 2015–2018 in a major urban area of the Sichuan Basin, Southwest China. *Earth Space Sci.* **2020**, *7*, e2020EA001194. [[CrossRef](#)]
56. Tao, J.; Zhang, L.; Engling, G.; Zhang, R.; Yang, Y.; Cao, J.; Zhu, C.; Wang, Q.; Luo, L. Chemical composition of PM<sub>2.5</sub> in an urban environment in Chengdu, China: Importance of springtime dust storms and biomass burning. *Atmos. Res.* **2013**, *122*, 270–283. [[CrossRef](#)]
57. Tao, J.; Gao, J.; Zhang, L.; Zhang, R.; Che, H.; Zhang, Z.; Lin, Z.; Jing, J.; Cao, J.; Hsu, S.C. PM<sub>2.5</sub> pollution in a megacity of southwest China: Source apportionment and implication. *Atmos. Chem. Phys.* **2014**, *14*, 8679–8699. [[CrossRef](#)]
58. Yao, X.H.; Chan, C.K.; Fang, M.; Cadle, S.; Chan, T.; Mulawa, P.; He, K.; Ye, B. The water-soluble ionic composition of PM<sub>2.5</sub> in Shanghai and Beijing, China. *Atmos. Environ.* **2002**, *36*, 4223–4234. [[CrossRef](#)]
59. Shen, Z.; Cao, J.; Arimoto, R.; Han, Y.; Zhu, C.; Tian, J.; Liu, S. Chemical characteristics of fine particles (PM<sub>1</sub>) from Xi'an, China. *Aerosol Sci. Technol.* **2010**, *44*, 461–472. [[CrossRef](#)]
60. Liu, P.; Ye, C.; Xue, C.; Zhang, C.; Mu, Y.; Sun, X. Formation mechanisms of atmospheric nitrate and sulfate during the winter haze pollution periods in Beijing: Gas-phase, heterogeneous and aqueous-phase chemistry. *Atmos. Chem. Phys.* **2020**, *20*, 4153–4165. [[CrossRef](#)]
61. Wang, Q.; Ding, H.; Yu, F.; Chao, N.; Li, Y.; Jiang, Q.; Huang, Y.; Duan, L.; Ji, Z.; Zhou, R.; et al. The characteristics and impact factors of sulfate and nitrate in urban PM<sub>2.5</sub> over typical cities of Hangzhou Bay area, China. *Atmosphere* **2023**, *14*, 1799. [[CrossRef](#)]
62. Cao, J.J.; Shen, Z.X.; Chow, J.C.; Qi, G.W.; Watson, J.G. Seasonal variations and sources of mass and chemical composition for PM<sub>10</sub> aerosol in Hangzhou, China. *Particuology* **2009**, *7*, 161–168. [[CrossRef](#)]
63. Xu, L.L.; Chen, X.Q.; Chen, J.S.; Zhang, F.W.; He, C.; Zhao, J.P.; Yin, L.Q. Seasonal variations and chemical compositions of PM<sub>2.5</sub> aerosol in the urban area of Fuzhou, China. *Atmos. Res.* **2012**, *104–105*, 264–272. [[CrossRef](#)]
64. Wang, X.; Bi, X.; Sheng, G.; Fu, J. Chemical composition and sources of PM<sub>10</sub> and PM<sub>2.5</sub> aerosols in Guangzhou, China. *Environ. Monit. Assess.* **2006**, *119*, 425–439. [[CrossRef](#)] [[PubMed](#)]
65. Wang, Y.; Zhuang, G.; Zhang, X.; Huang, K.; Xu, C.; Tang, A.; Chen, J.; An, Z. The ion chemistry, seasonal cycle, and sources of PM<sub>2.5</sub> and TSP aerosol in Shanghai. *Atmos. Environ.* **2006**, *40*, 2935–2952. [[CrossRef](#)]
66. Ohta, S.; Okita, T. A chemical characterization of atmospheric aerosol in Sapporo. *Atmos. Environ.* **1990**, *24*, 815–822. [[CrossRef](#)]
67. Duan, F.K.; Liu, X.D.; Yu, T.; Cachier, H. Identification and estimate of biomass burning contribution to the urban aerosol organic carbon concentrations in Beijing. *Atmos. Environ.* **2004**, *38*, 1275–1282. [[CrossRef](#)]
68. Peng, J.; Hu, M.; Shang, D.; Wu, Z.; Du, Z.; Tan, T.; Wang, Y.; Zhang, F.; Zhang, R. Explosive secondary aerosol formation during severe haze in the North China Plain. *Environ. Sci. Technol.* **2021**, *55*, 2189–2207. [[CrossRef](#)] [[PubMed](#)]
69. Cao, J.J.; Chow, J.C.; Watson, J.G.; Wu, F.; Han, Y.M.; Jin, Z.D.; Shen, Z.X.; An, Z.S. Size-differentiated source profiles for fugitive dust in the Chinese Loess Plateau. *Atmos. Environ.* **2008**, *42*, 2261–2275. [[CrossRef](#)]
70. Xiao, H.Y.; Liu, C.Q. Chemical characteristics of water-soluble components in TSP over Guiyang, SW China, 2003. *Atmos. Environ.* **2004**, *38*, 6297–6306. [[CrossRef](#)]
71. Zhang, R.J.; Cao, J.J.; Lee, S.C.; Shen, Z.X.; Ho, K.F. Carbonaceous aerosols in PM<sub>10</sub> and pollution gases in winter in Beijing. *J. Environ. Sci.* **2007**, *19*, 564–571. [[CrossRef](#)]
72. Cao, J.J.; Chow, J.C.; Tao, J.; Lee, S.C.; Watson, J.G.; Ho, K.F.; Wang, G.H.; Zhu, C.S.; Han, Y.M. Stable carbon isotopes in aerosols from Chinese cities: Influence of fossil fuels. *Atmos. Environ.* **2011**, *45*, 1359–1363. [[CrossRef](#)]
73. Dall'Osto, M.; Querol, X.; Alastuey, A.; O'Dowd, C.; Harrison, R.M.; Wenger, J.; Gómez-Moreno, F.J. On the spatial distribution and evolution of ultrafine particles in Barcelona. *Atmos. Chem. Phys.* **2013**, *13*, 741–759. [[CrossRef](#)]
74. Tian, H.; Wang, Y.; Xue, Z.; Qu, Y.; Chai, F.; Hao, J. Atmospheric emissions estimation of Hg, As, and Se from coal-fired power plants in China, 2007. *Sci. Total Environ.* **2011**, *409*, 3078–3081. [[CrossRef](#)] [[PubMed](#)]
75. Duc, H.N.; Bang, H.Q.; Quang, N.X. Modelling and prediction of air pollutant transport during the 2014 biomass burning and forest fires in peninsular Southeast Asia. *Environ. Monit. Assess.* **2016**, *188*, 106. [[CrossRef](#)] [[PubMed](#)]
76. Zhou, Y.; Xiao, H.; Guan, H.; Zheng, N.; Zhang, Z.; Tian, J.; Qu, L.; Zhao, J.; Xiao, H. Chemical composition and seasonal variations of PM<sub>2.5</sub> in an urban environment in Kunming, SW China: Importance of prevailing westerlies in cold season. *Atmos. Environ.* **2020**, *237*, 117704. [[CrossRef](#)]
77. Sofia, D.; Lotrecchiano, N.; Trucillo, P.; Giuliano, A.; Terrone, L. Novel air pollution measurement system based on ethereum blockchain. *J. Sens. Actuator Netw.* **2020**, *9*, 49. [[CrossRef](#)]

**Disclaimer/Publisher's Note:** The statements, opinions and data contained in all publications are solely those of the individual author(s) and contributor(s) and not of MDPI and/or the editor(s). MDPI and/or the editor(s) disclaim responsibility for any injury to people or property resulting from any ideas, methods, instructions or products referred to in the content.